Cell Tissue Res (2005) 321: 21–33
DOI 10.1007/s00441-005-1111-y

REGULAR ARTICLE

I. Pintelon · I. De Proost · I. Brouns · H. Van Herck · J. Van Genechten · F. Van Meir · J.-P. Timmermans · D. Adriaensen

Selective visualisation of neuroepithelial bodies in vibratome slices of living lung by 4-Di-2-ASP in various animal species

Received: 21 December 2004 / Accepted: 1 March 2005 / Published online: 19 May 2005

Abstract Pulmonary neuroepithelial bodies (NEBs) are extensively innervated organoid groups of neuroendocrine cells that lie in the epithelium of intrapulmonary airways. Our present understanding of the morphology of NEBs is comprehensive, but direct physiological studies have so far been challenging because the extremely diffuse distribution of NEBs makes them inaccessible in vivo and because a reliable in vitro model is lacking. Our aim has been to optimise an in vitro method based on vibratome slices of living lungs, a model that includes NEBs, the surrounding tissues and at least part of their complex innervation. This in vitro model offers satisfactory access to pulmonary NEBs, provided that they can be differentiated from other tissue elements. The model was first optimised for living rat lung slices. Neutral red staining, reported to stain rabbit NEBs, proved unsuccessful in rat slices. On the other hand, the styryl pyridinium dye, 4-(4-diethylaminostyryl)-*N*-methylpyridinium iodide (4-Di-2-ASP), showed brightly fluorescent cell groups, reminiscent of NEBs, in the airway epithelium of living lung slices from rat. In addition, nerve fibres innervating the NEBs were labelled. The reliable and specific labelling of pulmonary NEBs by 4-Di-2-ASP was corroborated by immunostaining for protein gene-product 9.5. Live cell imaging and propidium iodide staining further established the acceptable viability of 4-Di-2-ASP-labelled NEB cells in lung slices, even over long periods. Importantly, the in vitro model and 4-Di-2-ASP staining procedure for pulmonary NEBs appeared to be equally reproducible in mouse, hamster and rabbit lungs. Diverse immunocytochemical procedures could be applied to the lung slices providing an opportunity to combine physiological and functional morphological studies. Such an integrated approach offers additional possibilities for elucidating the function(s) of pulmonary NEBs in health and disease.

Keywords 4-Di-2-ASP · Styryl pyridinium dyes · Neuroepithelial bodies · Lung · Rat (Wistar) · Syrian hamster · Swiss mice

This work was supported by the following research grants: Fund for Scientific Research Flanders (G.0155.01 to D.A.), NOI-BOF (to D.A.) and BOF-RUCA Small Projects (KPO2 to D.A., I.B. and F.V.M.) from the University of Antwerp.

I. Pintelon · I. De Proost · I. Brouns · H. Van Herck · J. Van Genechten · F. Van Meir · J.-P. Timmermans · D. Adriaensen (✉)
Department of Biomedical Sciences,
Laboratory of Cell Biology and Histology,
University of Antwerp,
Groenenborgerlaan 171,
2020 Antwerp, Belgium
e-mail: dirk.adriaensen@ua.ac.be
Tel.: +32-3-2653475
Fax: +32-3-2653301

Introduction

Pulmonary neuroepithelial bodies (NEBs; Lauweryns and Peuskens 1972) are organoid clusters of neuroendocrine cells located in the epithelium of intrapulmonary airways (for reviews, see Scheuermann 1987; Sorokin and Hoyt 1989; Adriaensen and Scheuermann 1993; Adriaensen et al. 2003). All NEBs are characterised by dense-cored secretory granules that contain bioactive substances, such as monoamine, peptide and purine transmitters (for reviews, see Sorokin and Hoyt 1989; Adriaensen and Scheuermann 1993; Adriaensen and Timmermans 2004). Furthermore, multiple nerve fibre populations provide extensive innervation in which sensory and motor terminals have been reported to contact pulmonary NEBs (Sorokin and Hoyt 1989; Adriaensen et al. 2003; Brouns et al. 2004).

Although many, mainly morphological, data are supportive of a role for NEBs as complex intraepithelial airway receptors, conclusive physiological data on their exact function are still lacking. In many species, NEBs share a preferential localisation at or near airway bifurcations, strategically located for sensing changes in the airway gas concentration (Cho et al. 1989). Although in vitro physiological experiments, mainly performed on isolated pulmonary neuroendocrine cells (PNECs) and small cell lung carcinoma (SCLC) cell lines, suggest the presence of a

functional system for oxygen-sensing in NEBs (Youngson et al. 1993, 1997a,b; Cutz and Jackson 1999; Peers and Kemp 2001; Kemp et al. 2002), the exact nature of the physiological stimulus modality of NEB cells in healthy lungs is still unknown. In view of the presence of a wide variety of different physiologically characterised airway receptors (for a review, see Widdicombe 2001), pulmonary NEBs connected to vagal sensory nerve terminals have been suggested to act as mechanoreceptors (Lauweryns and Peuskens 1972; Wasano and Yamamoto 1978; Brouns et al. 2003b, 2004).

Direct physiological studies of pulmonary NEBs are difficult to perform, because NEBs are diffusely distributed in the lung parenchyma and represent only a minor fraction of the population of airway epithelial cells. Therefore, pulmonary NEBs are almost inaccessible for direct measurements and manipulation. In vitro models of PNECs include organ cultures (Carabba et al. 1985), isolated PNECs (Cutz et al. 1985; Speirs et al. 1992; Speirs and Cutz 1993), SCLC lines and, more recently, fresh vibratome slices (Fu et al. 1999). Cultures of isolated PNECs have the disadvantage that they are difficult to reproduce and that the cells are completely isolated from their in vivo surroundings. Because of the extensive innervation of pulmonary NEBs (Adriaensen et al. 2003) and because of the probable modulatory influence of innervation (Lauweryns and Van Lommel 1986) and environment on NEB cells, the use of fresh lung slices that include NEBs, the surrounding tissues and at least part of their innervation seems to be a better model for studying NEBs in vitro.

A precondition for performing physiological experiments on the diffusely distributed pulmonary NEBs is the ability to visualise them. In living slices of, in particular, rabbit lungs, NEBs have been reported to be identifiable by vital staining with neutral red (Fu et al. 1999, 2002). Styryl pyridinium dyes seem to be good candidates for the vital staining of NEBs in fresh lung slices, especially 4-(4-diethylaminostyryl)-*N*-methylpyridinium iodide (4-Di-2-ASP), which appears to label neuroendocrine cells specifically in the skin (Nurse and Farraway 1989). Originally, 4-Di-2-ASP was used to visualise motor nerve terminals (Kelly et al. 1985; Magrassi et al. 1987; Lichtman et al. 1987; Herrera and Banner 1990), nerve fibres in autonomic ganglia (Hanani 1992) and neuronal cell bodies in the choroid (Bergua et al. 1994; Schrödl et al. 2003), the enteric nervous system (Cornelissen et al. 1996) and the gallbladder (Hillsley et al. 1998). Whereas its exact staining mechanism is still unclear, 4-Di-2-ASP is known to be taken up in the plasma membrane and later on in mitochondria of living excitable cells (Loew et al. 1985).

The aim of the present study has been to optimise a slice model for rat lungs, because a vast body of morphological data is available about NEBs and their extremely complex innervation in Wistar rats (Adriaensen et al. 2003). Moreover, this model can be used to study other rat strains, e.g. the fawn–hooded rat, which shows a congenital predisposition to primary pulmonary hypertension and an altered nitrergic innervation of pulmonary NEBs (Van Genechten et al. 2004). Since no reliable methods have previously been available to visualise NEBs in rat lung slices, the present study has explored the possibilities of neutral red and 4-Di-2-ASP as selective vital labels for pulmonary NEBs. The efficacy of 4-Di-2-ASP for staining pulmonary NEBs has also been tested in mice, hamsters and rabbits. Because a combined physiological and morphological approach is generally considered to be the most effective, the living lung slice model has also been evaluated for its possible use in further investigations of functionally characterised NEBs by immunocytochemical staining protocols.

Materials and methods

Animals

Lung tissue was obtained from 1- to 10-day-old (postnatal day 1–10, PD1-10) Wistar rats (n=12), Swiss mice (n=10) and Syrian hamsters (n=2) and from 4-week-old New Zealand white rabbits (n=2; Charles River, Brussels, Belgium) of both sexes. Rabbits and newborn animals with their mothers were kept in acrylic cages in an acclimatised room (12/12 h light/dark cycle; 22±3°C) and were provided with water and food ad libitum. National and international principles of laboratory animal care were followed and the experiments were approved by the local ethics committee of the University of Antwerp.

Preparation of lung slices

All animals were killed by intraperitoneal injection of an overdose of sodium pentobarbital (Nembutal 200 mg/kg, CEVA Santé Animale, Brussels, Belgium) containing heparin (500 U/kg; Rhône Poulenc Rorer 256S68F12; Brussels, Belgium). The pulmonary circulation was perfused via the right ventricle with an oxygenated (95% O_2, 5% CO_2) Krebs solution (118 mM NaCl, 4.75 mM KCl, 2.54 mM $CaCl_2.2H_2O$, 1.2 mM $MgSO_4.7H_2O$, 1 mM $NaH_2PO_4.2H_2O$, 25 mM $NaHCO_3$, 11.1 mM D-glucose, pH 7.4 adjusted with HCl). Lung tissue was stabilised by slowly instilling a 2% agarose solution (low-melt agarose, A4018, Sigma, Bornem, Belgium) via a tracheal cannula. After inflation, lungs were dissected and transferred to ice-cold oxygenated Krebs to enable the complete gelling of the agarose. Slices (200–300 μm thick) of each lung lobe were cut by using a vibratome (Microm, HM650 V, Microm International, Walldorf, Germany) and 10–15 slices per animal were subsequently kept in oxygenated ice-cold Krebs solution until further manipulation.

Vital neutral red staining of lung slices and administration of 5-HT precursors

As previously described (Fu et al. 1999), lung slices of mice (n=7) and rats (n=10) were incubated with neutral red (N4638, Sigma, Bornem, Belgium) at concentrations

ranging from 0.001 mg/ml to 0.06 mg/ml in Dulbecco's modified Eagle's medium/F-12 (DMEM-F-12, Gibco, Invitrogen, Merelbeke, Belgium) over time periods of 5–120 min at 37°C.

Some animals were pretreated with 5-hydroxytryptophan (5-HTP; H9772, Sigma, Bornem, Belgium), a 5-HT precursor, in two different ways. First, pregnant mice (n=4) received a daily injection of 5-HTP (50 mg/kg body weight) during the last 3 days of gestation. Lung slices were taken from the offspring (n=7) during the first few days after the treated animals had given birth. Second, neonatal rats (n=5) and mice (n=5) were injected with 5-HTP (100 mg/kg body weight) 1 h before dissection. Lung slices of pretreated animals were subjected to identical staining procedures as slices without pretreatment.

Staining with 4-Di-2-ASP

Lung slices were incubated for 5–30 min with 4 μM 4-Di-2-ASP (D-289, Molecular Probes, Invitrogen, Merelbeke, Belgium) in DMEM-F-12 at 37°C. Slices were rinsed in DMEM-F-12 at 37°C and subsequently analysed by means of an epi-fluorescence microscope (Zeiss Axiophot) equipped with appropriate filters (Zeiss 17; BP485-20/FT 510/BP 515–565).

Viability test with propidium iodide

To test the viability of the lung slices, propidium iodide (PI) was used to mark dead cells or cells with damaged membranes, the nuclei of which show red fluorescence after PI staining. Living cells with intact cell membranes are impermeable to PI and will not exhibit nuclear staining. At different time points after 4-Di-2-ASP staining, lung slices (n=15; from five rats) were incubated for 1 min in 5 μM PI (P-4170, Sigma, Bornem, Belgium) in DMEM-F-12 and subsequently rinsed for 15 min in DMEM-F-12.

Immunocytochemistry on lung slices

Because 4-Di-2-ASP fluorescence disappears after fixation, staining was first localised and imaged in living lung slices. Subsequently, the slices were fixed for 3 h in 4% paraformaldehyde (0.1 M phosphate buffer, pH 7.4) and immunostained for protein gene-product 9.5 (PGP9.5), a general marker for neuronal and neuroendocrine tissues. To this end, slices (n=72, from 12 rats; n=55, from 10 mice; n=11, from 2 hamsters) were subjected to an immunocytochemical staining protocol with rabbit polyclonal antibodies against PGP9.5 (1/4,000; overnight; room temperature; Biogenesis 7863-0504, Poole, UK) and red-fluorescent (Cy3) conjugated Fab fragments of goat anti-rabbit immunoglobulins (1/2,000; 4 h; room temperature; Jackson Immunoresearch 111-167-003, West grove, Pa., USA). Primary and secondary antisera were diluted in phosphate-buffered saline (PBS) containing 10% normal goat serum, 0.1% bovine serum albumin, 0.05% thimerosal and 0.01% NaN_3 (PBS*). Prior to incubation with the primary antisera, lung slices were incubated for 1 h with PBS* containing 1% Triton X-100.

Tyramide signal amplification (TSA)-enhanced immunostaining with rabbit polyclonal antibodies against the ATP receptor $P2X_3$ (gift from Roche Bioscience, Palo Alto, Calif., USA; see Brouns et al. 2000) and subsequent double-labelling for PGP9.5 were performed on fixed lung slices (n=6; from 3 rats) as previously described for 20-μm-thick cryostat sections of rat lungs (Brouns et al. 2000). Slight modifications of the original procedure were, however, needed to optimise the protocol for 200– to 300-μm-thick lung slice preparations. Endogenous peroxidase activity was blocked by incubating the lung slices for 30 min in a 3% H_2O_2 solution in ultrapure H_2O. $P2X_3$ immunoreactivity was visualised in lung slices by using Cy3-conjugated streptavidin (1/6,000; 1 h; room temperature; Jackson Immunoresearch 016-160-084), whereas fluorescein isothiocyanate (FITC)-conjugated Fab fragments of goat anti-rabbit immunoglobulins (1/2,000; 4 h; room temperature; Jackson Immunoresearch 111-097-003) were used to detect the PGP9.5 antibody.

Microscopic analysis

Neutral red staining in lung slices was imaged by using an Olympus BX50 microscope (Olympus, Tokyo, Japan) equipped with a Sony charge-coupled device camera (Sony Power, Tokyo, Japan) and analySIS 2.1 software (Soft Imaging System, Münster, Germany).

To obtain detailed images of the 4-Di-2-ASP staining in living slices and of the immunocytochemical labelling in fixed lung slices, a microlens-enhanced dual spinning disk confocal microscope (UltraVIEW Live Cell Imager (LCI), PerkinElmer, Seer Green, UK), equipped with a three-line (488, 568 and 647 nm) argon–krypton laser was used. 4-Di-2-ASP (excitation maximum: 488 nm; emission maximum: 607 nm) was excited by the 488-nm line and the fluorescence was recorded using a 500-nm longpass filter.

In order to use the labelled lung slices in physiological "live cell imaging" experiments, lung slices were transferred to a perfusion chamber mounted on the stage of the microscope (Axiovert 200, Zeiss) of the UltraVIEW LCI and were continuously perfused with an oxygenated Krebs solution at a rate of 5 ml/min. High-resolution time-lapse images (10 images/s, 1344×1024 pixels) of the intracellular 4-Di-2-ASP fluorescence in pulmonary NEBs (n=10; in 7 slices from 3 rats) were captured in one confocal plane under constant illumination over a time period of 5 min by using a ×63 oil immersion objective.

In a second experiment, time-lapse images were registered in one confocal plane for 10 min (5 images/s), again under constant illumination, to evaluate possible cytotoxic effects of 4-Di-2-ASP excitation or emission light. In total, 5 NEBs were evaluated in 4 slices of 2 different rats. Image data were analysed off-line by Volocity2 software (Improvision, Coventry, UK).

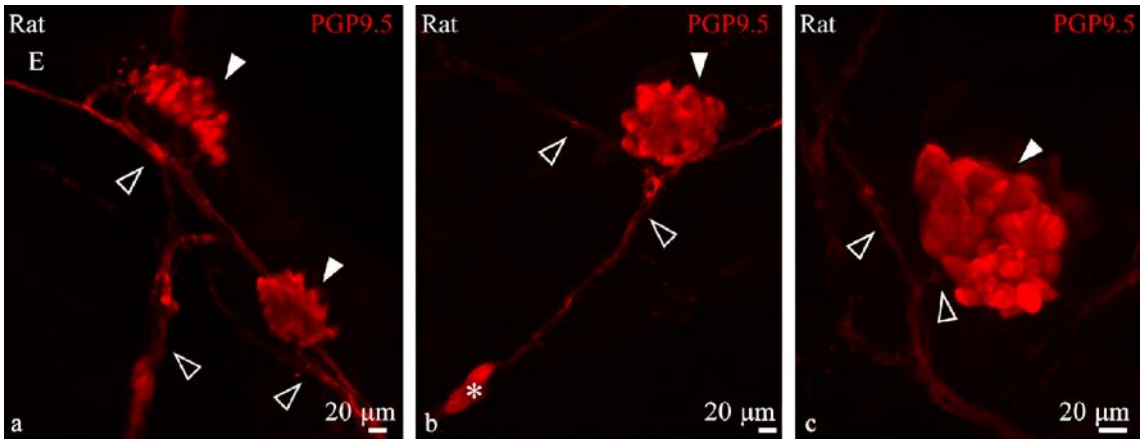

Fig. 1 **a**–**c** Vibratome slices (200 µm) of lung lobes of a 2-day-old rat, fixed and immunostained for protein gene-product 9.5 (PGP9.5). Confocal images show pulmonary NEBs (*arrowheads*) located in the epithelial lining (*E*) of bronchioles. In addition, dense networks of nerve fibres (*open arrowheads*) and nerve terminals are seen to contact the pulmonary NEBs. **a** Two PGP9.5-immunoreactive (IR) NEBs, contacted by a complex network of nerve fibres. Projection of 21 confocal images (2-µm intervals). **b** Pulmonary NEB receiving several nerve fibres. Note a neuronal cell body (*asterisk*) located close to the NEB. Projection of eight confocal images (5-µm intervals). **c** High-magnification image of a PGP9.5-IR NEB. Distinct PGP9.5-IR nerve terminals, related to the NEB are suggestive of a complex innervation. Projection of 54 confocal images (1-µm intervals)

Results

Evaluation of lung slices as a possible model for functional studies of NEBs

Immunocytochemical staining for the general neuronal and neuroendocrine marker PGP9.5 on 200– to 300-µm-thick fixed lung slices revealed a number of pulmonary NEBs in all slices of neonatal animals (Fig. 1a–c). For example, approximately 30 and 20 NEBs could be found in every lung slice of rats at PD5 and PD10, respectively. In addition, PGP9.5-immunoreactive (IR) nerve bundles and fibres were also seen in these lung slices, some of which clearly contacted PGP9.5-IR NEBs (Fig. 1a–c). Occasionally, the latter seemed to arise from neuronal cell bodies that could be found close to NEBs in the lung slices (Fig. 1b).

Neutral red staining of living lung slices of rats and mice

Neutral red staining of living rat and murine lung slices did not result in a reproducible visualisation of NEBs. After incubation of rat lung slices with neutral red, many macrophages appeared to have taken up the dye and were

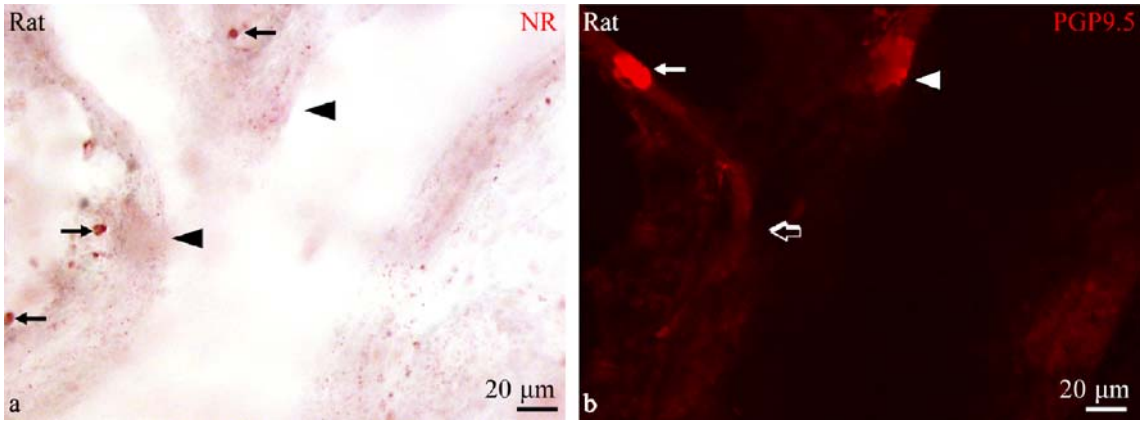

Fig. 2 Neutral red (*NR*) staining of a living rat (postnatal day 3; PD3) lung slice (**a**), subsequently fixed and immunostained for PGP9.5 (**b**). After incubation with neutral red, dark red stained macrophages (*arrows*) are clearly distinguishable in the lung slices (**a**). In contrast, pinkish red staining is occasionally seen in the epithelium (*arrowheads*) suggestive of labelled epithelial cell groups. Although neutral red staining was abolished after fixation with paraformaldehyde (**b**), the area imaged in **a** could be traced back after subsequent immunostaining for PGP9.5, revealing the location of two pulmonary NEBs in the imaged region. Apparently one of the intraepithelial cell groups that were seen to be faintly stained with neutral red in **a** corresponds to the presence of a pulmonary NEB (*white arrowhead*), whereas other stained areas do not (*open arrow*). Moreover, the second NEB (*white arrow*) is not associated with the neutral red staining in **a**.

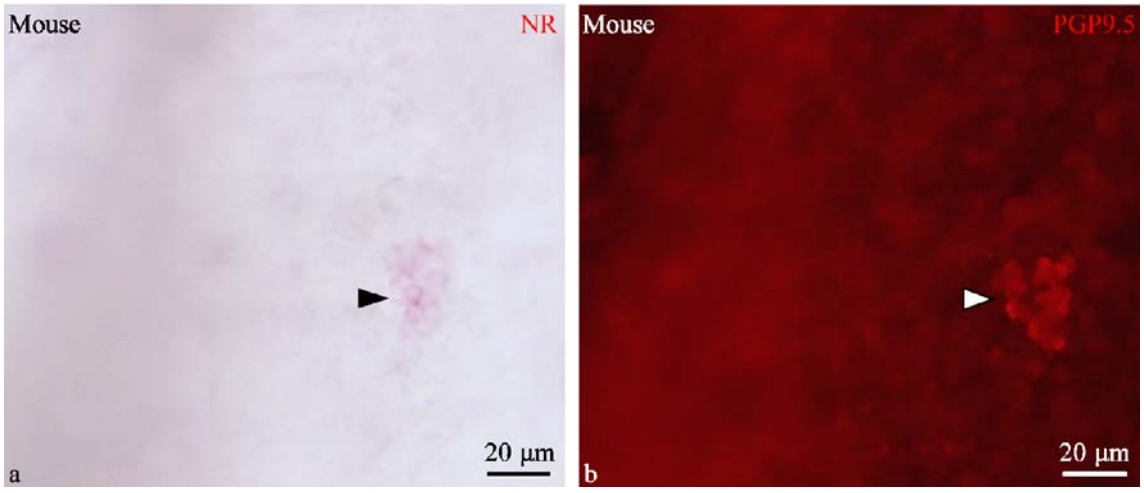

Fig. 3 Lung slice of a mouse (PD3) pre-treated with 5-HTP and stained in vitro with neutral red (**a**), followed by fixation and immunocytochemical staining for PGP9.5 (**b**). Detail of a weakly neutral red-stained cell group (*arrowhead* in **a**). A PGP9.5-IR NEB (*white arrowhead* in **b**) colocalises with the stained cell group in **a**.

consequently clearly distinguishable in the lung slices (Fig. 2a). In contrast, faint red staining could sporadically be noticed in the epithelium, suggestive of labelled intraepithelial cell groups (Fig. 2a). Although neutral red staining was abolished after fixation with paraformaldehyde, the same areas as those imaged with the neutral red staining could be traced back after fixation and subsequent immunostaining for PGP9.5 applied to localise pulmonary NEBs in the lung slices (Fig. 2b). The weak pinkish labelling that was sometimes seen in the epithelium after neutral red staining appeared to correspond to the presence of pulmonary NEBs only to a certain extent, since the stained areas did not always coincide with a PGP9.5-IR pulmonary NEB (Fig. 2a, b). Even after numerous trials of modifications of the original procedure, neutral red staining was mainly seen in macrophages and was apparently not able to provide reproducible labelling of intraepithelial cell groups. NEBs could not be distinguished unambiguously under any conditions.

In living lung slices of 5-HTP-pretreated mice (Fig. 3a, b), a few NEBs revealed more clear neutral red (0.02 mg/ml for 20 min) staining (Fig. 3a), which was, however, difficult to reproduce. Pretreatment of rats did not result in reproducible clear neutral red staining of NEBs in lung slices.

In vitro 4-Di-2-ASP staining of rat lung slices

Observation of the lung slices at various time intervals after incubation with 4-Di-2-ASP yielded distinct fluorescent images. Immediately after incubation, networks of fluo-

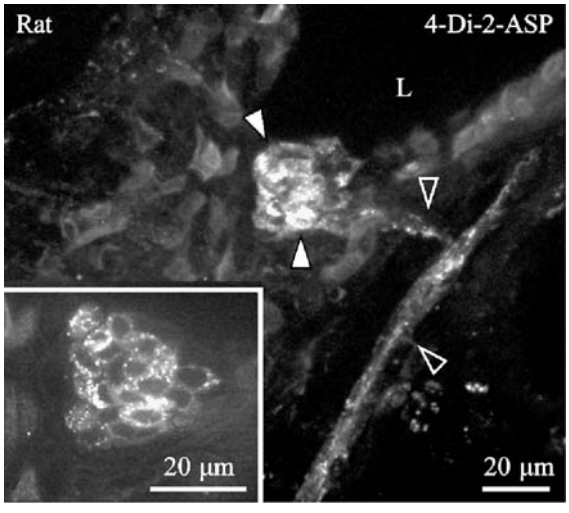

Fig. 4 Incubation of a living rat (PD7) lung slice with 4-Di-2-ASP reveals nerve fibres (*open arrowheads*), related to a 4-Di-2-ASP-fluorescent cell group (*white arrowheads*) in a bronchiole (*L* lumen bronchiole). Projection of 35 confocal images (1-µm intervals). *Insert*: Higher magnification of just one confocal plane of the same cell group, revealing the granular staining pattern of 4-Di-2-ASP

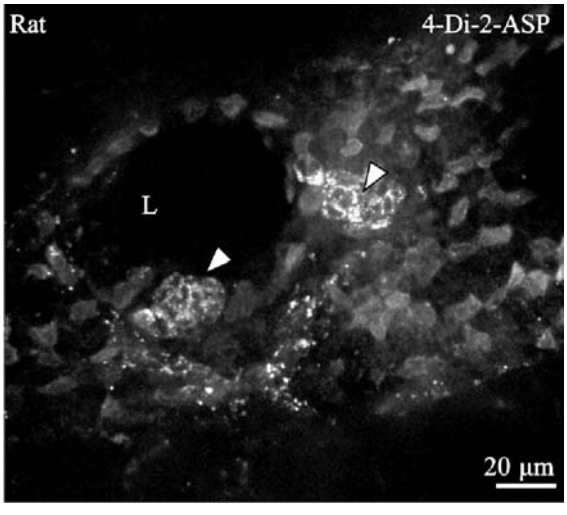

Fig. 5 The vital dye 4-Di-2-ASP appears to be specifically taken up by two groups of epithelial cells (*arrowheads*) in a bronchiole of a living rat (PD7) lung slice (*L* lumen bronchiole). Projection of 25 confocal images (1-µm intervals)

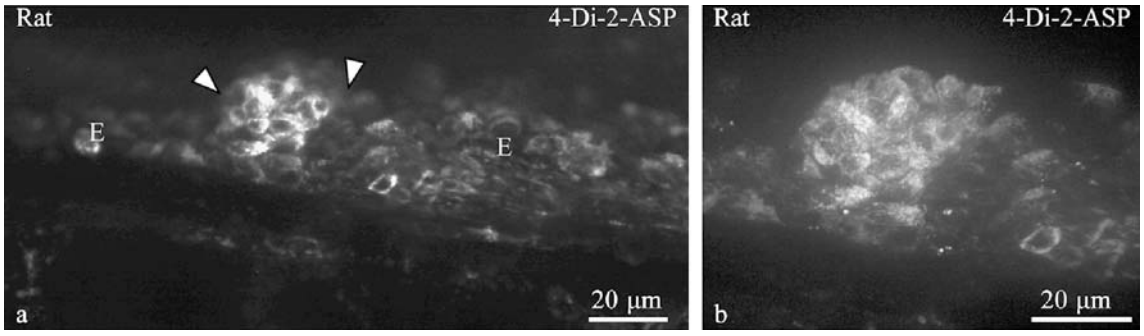

Fig. 6 **a** Overview of a longitudinal section of the epithelial (*E*) lining of a bronchus in a living rat (PD2) lung slice, showing a fluorescent cell group (*arrowheads*) after incubation with the vital dye 4-Di-2-ASP. **b** High-magnification detail of the 4-Di-2-ASP-labelled cell group shown in **a**. Projection of 51 confocal images (0.5-µm intervals)

rescent nerve bundles were seen to traverse the airway walls. Two hours later, a slight reduction in fluorescence intensity in the nerve fibres (Fig. 4) was accompanied by a gradual uptake of 4-Di-2-ASP by groups of epithelial cells in the airways. After the slices had been rinsed for 4 h, brightly 4-Di-2-ASP fluorescent cell groups could be seen in the airway epithelium of all rat lung slices (Figs. 4, 5, 6). Similar fluorescent cell groups were present in the epithelium of bronchi and bronchioli but could also be observed in the respiratory areas.

Fluorescent 4-Di-2-ASP was typically found as a granular staining pattern in the labelled epithelial cells (Fig. 4). Once the dye had been incorporated into the epithelial cells, fluorescence was detectable for at least 24 h after initial staining of the lung slice.

In addition to the obvious staining of nerve fibres and intraepithelial cell groups, 4-Di-2-ASP fluorescence was also seen in groups of subepithelial cells in the airway walls. These cells were larger than the stained epithelial cells and revealed large unstained nuclei, suggestive of neurons in intrinsic ganglia, which were sometimes seen close to NEBs in the lung slices.

Identification of intraepithelial 4-Di-2-ASP-labelled cell groups in rat lung slices as pulmonary NEBs

The localisation and morphology of the 4-Di-2-ASP-stained intraepithelial cell groups were reminiscent of the presence of NEBs. To establish that these cells were indeed one and the same, fluorescent cell groups were imaged in the confocal microscope, with lung slices subsequently being fixed and immunostained for PGP9.5. Correlation of the PGP9.5-IR NEBs and the 4-Di-2-ASP-labelled cell groups in rats (Figs. 7, 8) revealed that all intraepithelial cell groups that had been identified by 4-Di-2-ASP unambiguously corresponded to PGP9.5-IR pulmonary NEBs.

Viability of pulmonary NEBs in rat lung slices after 4-Di-2-ASP labelling and long-term fluorescent excitation

Staining with PI did not reveal nuclear staining in any of the 4-Di-2-ASP-labelled NEBs in rat lung slices, even up to

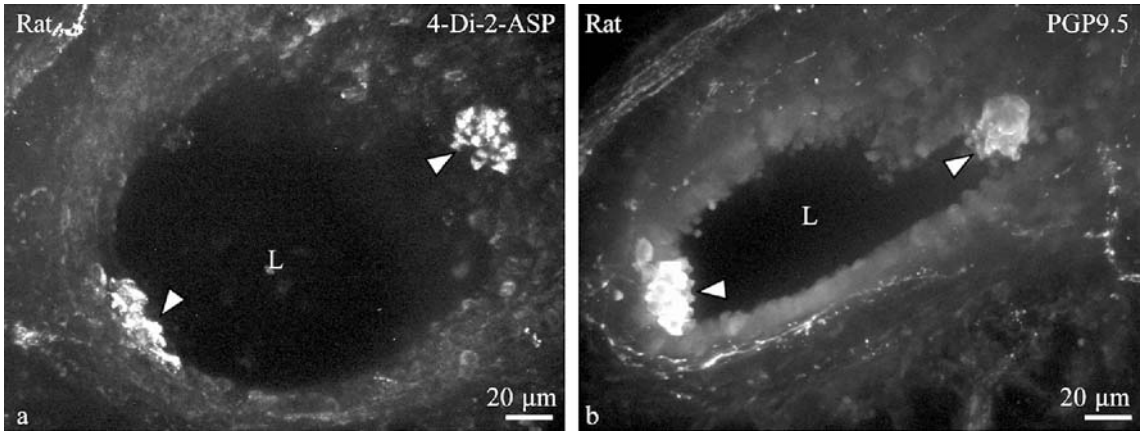

Fig. 7 **a** Cross section of a bronchiole in a rat (PD3) lung slice, showing two strongly 4-Di-2-ASP-fluorescent intraepithelial cell groups (*arrowheads*), suggestive of the presence of pulmonary NEBs (*L* lumen bronchiole). Projection of 60 confocal images (0.5-µm intervals). **b** Same bronchiole after fixation and PGP9.5 immunostaining, illustrating that both cell groups identified in **a** indeed correspond to PGP9.5-IR pulmonary NEBs (*arrowheads*). Note the morphological changes of the airway in the lung slice caused by fixation. Projection of 100 confocal images (0.5-µm intervals)

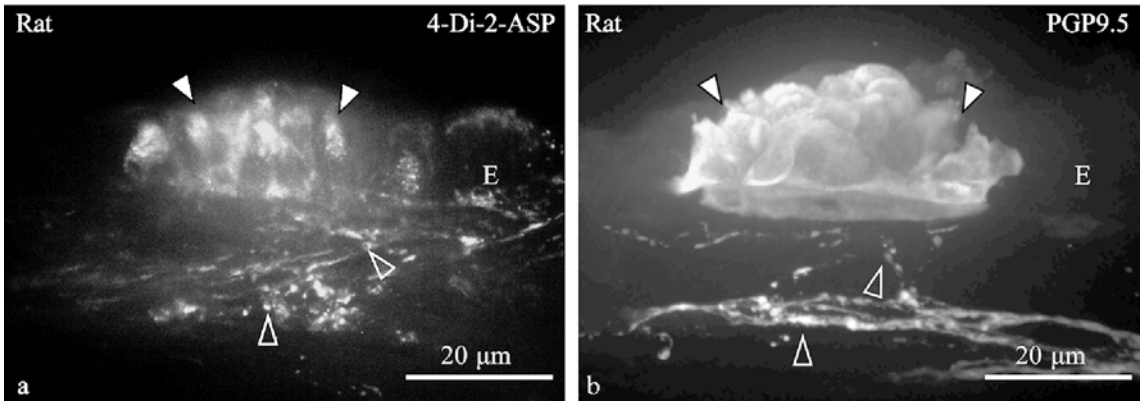

Fig. 8 High-magnification detail of a cross section of the wall of a bronchus in a rat (PD2) lung slice. **a** A 4-Di-2-ASP-fluorescent cell group (*white arrowheads*) is seen in the epithelium (*E*) after incubation with the vital dye. Note that the nerve fibres (*open arrowheads*) contacting the labelled cell group are also stained with 4-Di-2-ASP. Projection of 33 confocal images (0.5-µm intervals). **b** Identical region of the lung slice as imaged in **a** after fixation and immunostaining for PGP9.5, clearly revealing that the 4-Di-2-ASP-labelled cell group colocalises with a PGP9.5-IR pulmonary NEB. Projection of 71 confocal images (0.5-µm intervals)

8 h after 4-Di-2-ASP incubation (Fig. 9). PI-stained nuclei were also rare in other airway epithelial cells. Nuclear PI staining was, however, observed in some of the neighbouring pneumocytes and smooth muscle cells.

Fluorescent 4-Di-2-ASP generally displayed a granular staining pattern in the labelled NEB cells. Time-lapse movies recorded by using the dual spinning disk confocal UltraVIEW LCI (PerkinElmer) revealed that the fluorescent granules represented cell organelles undergoing rapid movements in the cytoplasm of the labelled cells (Fig. 10a–c). Additionally, coordinated ciliary beats could be observed in ciliated epithelial cells that neighboured NEBs, for at least 24 h after 4-Di-2-ASP staining.

No direct negative effect on the viability of pulmonary NEBs was observed by 4-Di-2-ASP staining. Possible phototoxic effects of the exposure to fluorescence emission light and, especially, excitation light were assessed. By using the conditions of the confocal microscope that were consistent with our experimental set-up for live-cell imaging, selected NEBs were illuminated continuously for 10 min. Before and after illumination, PI staining was performed to evaluate the viability of the investigated NEBs. NEB cells that showed good viability before illumination (Fig. 11a) never exhibited nuclear PI staining after exposure to laser light (Fig. 11b). No obvious phototoxic effects were observed.

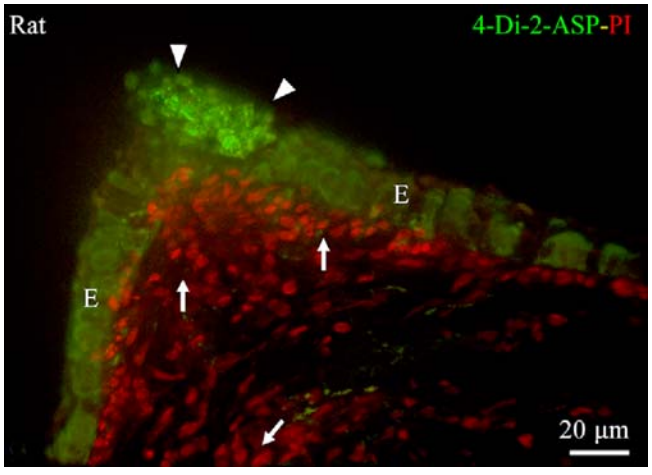

Fig. 9 Rat lung slice taken from an 8-day-old animal (*E* bronchial epithelium) and stained with propidium iodide (PI; *red* fluorescence), 8 h after 4-Di-2ASP labelling (*green* fluorescence). Staining with PI did not result in nuclear staining of any of the cells in the imaged 4-Di-2-ASP-labelled bronchial NEB (*arrowheads*). Nuclear PI staining was however observed in a number of neighbouring cells in the airway wall and in alveolar areas (*arrows*). Projection of 30 confocal images (1-µm intervals)

Immunocytochemical staining of agarose-filled lung slices

The ATP receptor $P2X_3$, known to be expressed on vagal sensory nerve fibres selectively contacting pulmonary NEBs (Brouns et al. 2000, 2003a), could be demonstrated in fixed rat lung slices by using TSA-enhanced immunocytochemical staining. A slight modification of the procedure for cryostat sections resulted in the visualisation of $P2X_3$ receptor-IR nerve fibres that were seen to traverse the airway walls, thereby regularly giving rise to extensive intraepithelial arborisations. Subsequent labelling of the lung slices processed for $P2X_3$ localisation, with an antibody against PGP9.5 revealed that intraepithelial $P2X_3$ receptor-IR nerve terminals in all cases coincided with the presence of a PGP9.5-IR NEB (Fig. 12a–d).

Efficacy of 4-Di-2-ASP staining in other laboratory animal species

To test the efficacy of 4-Di-2-ASP for the selective staining of pulmonary NEBs in various species, the dye was used to stain lung slices of mice (Fig. 13), hamsters (Fig. 14) and rabbits (Fig. 15).

In all species examined, 4-Di-2-ASP was seen to mark cell groups in the epithelium of the lung selectively. The rate of 4-Di-2-ASP uptake by the epithelial cells, however,

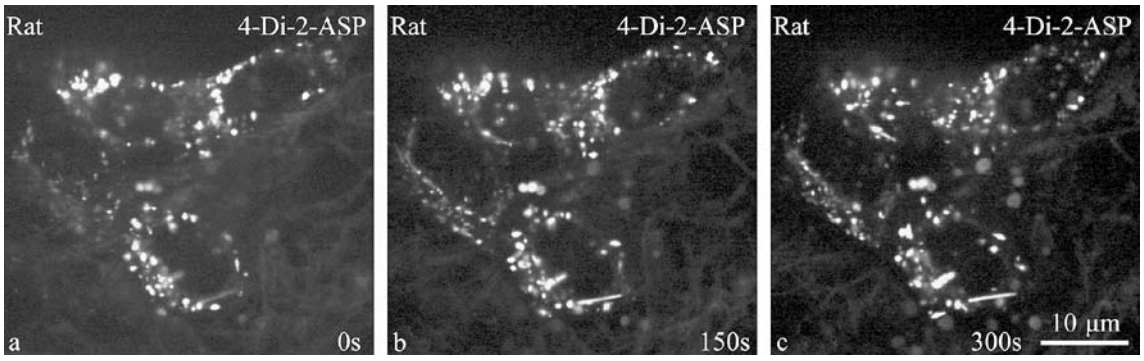

Fig. 10 Live-cell imaging of the rapid movements of the granular 4-Di-2-ASP fluorescence in NEB cells in a rat lung slice (PD10), 24 h after staining. Three single images taken from a time-lapse series (3,000 images in 5 min) captured by using an UltraVIEW confocal live cell imager (PerkinElmer) and representative of the observed rapid movements of fluorescent granules in the cytoplasm of labelled cells. As 4-Di-2-ASP is presumed to be taken up by mitochondria, the revealed movement may be considered to correspond to high activity of the mitochondria, indicating that the stained NEB cells in lung slices are viable and healthy. **a** Time point: 0 s. **b** Time point: 150 s **c** Time point 300 s

seemed to be species-dependent. In hamsters, 4-Di-2-ASP-labelled cells could be detected in less than 1 h after 4-Di-2-ASP incubation, whereas in mice, the time for the additional wash in culture medium needed to be extended up to 6 h. In lung slices of the rabbit, fluorescent cells were visible 4 h after staining, as in the rat. PGP9.5 immunostaining on fixed lung slices confirmed that 4-Di-2-ASP-labelled cell groups in the epithelium coincided unequivocally with the presence of a pulmonary NEB (Figs. 16, 17). In addition, some of the nerve fibres (Fig. 13) and presumed intrinsic ganglionic neurons (Fig. 18) could be visualised with 4-Di-2-ASP in the lung slices of all studied species. In none of the species did structures other than the intraepithelial cell groups and neuronal tissues display selective 4-Di-2-ASP fluorescence.

As in rats, labelled NEBs did not show nuclear propidium iodide (PI) staining 8 h after 4-Di-2-ASP incubation (Fig. 19), indicating that this dye does not negatively affect cell viability.

Discussion

The in vitro model optimised in this study involves the use of 4-Di-2-ASP to visualise NEBs in living lung slices of rats and of diverse animal species that are also important for the investigation of NEBs. In situ 4-Di-2-ASP-stained NEBs have been recognised unequivocally in the airway epithelium of all the species that we have examined. Moreover, following our in vitro studies, lung slices can easily be further processed for morphological examination.

The use of agarose-embedded lung slices to perform physiological studies, especially on rabbit NEBs, has been reported earlier (Fu et al. 1999, 2002). Since lung slices are much easier to prepare than dissociated cell cultures, the technique should facilitate comparative studies of NEB responses (Fu et al. 1999). This fresh lung slice technique also allows physiological recording from NEB cells, without potential artefacts induced by enzymatic treatment, cell dissociation and/or long-term culture (Fu et al. 1999).

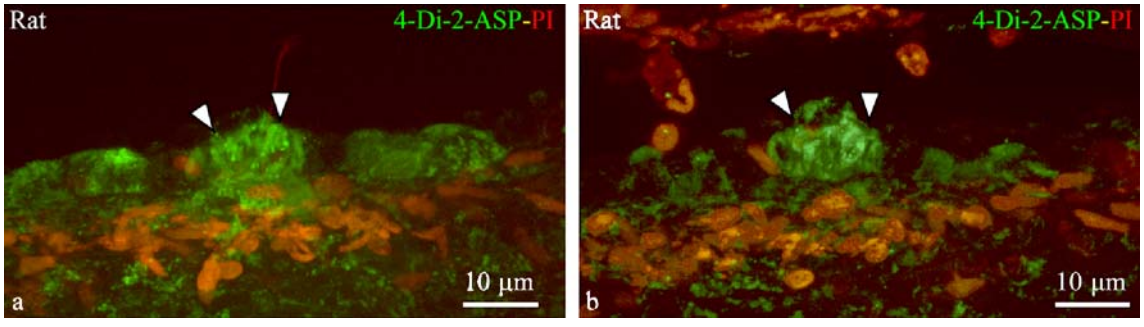

Fig. 11 PI staining of a living lung slice of a 2-day-old rat, before (**a**) and after (**b**) excitation (488 nm laser light) of a 4-Di-2-ASP-labelled NEB (*arrowheads*). Conditions used for illumination were representative for our experimental live-cell imaging set-up. This bronchiolar NEB was illuminated continuously for 10 min, while images were captured in one confocal plane. **a** The lung slice was stained with PI, 9 h after 4-Di-2-ASP labelling and imaged before the 10-min illumination. No nuclear PI staining could be observed in the 4-Di-2-ASP-fluorescent NEB, confirming the good viability of the cells. **b** After time-lapse imaging, the same NEB was apparently still devoid of nuclear PI staining, strongly indicating that excitation of the 4-Di-2-ASP in the NEB cells had no adverse effects on the viability of the labelled cells.

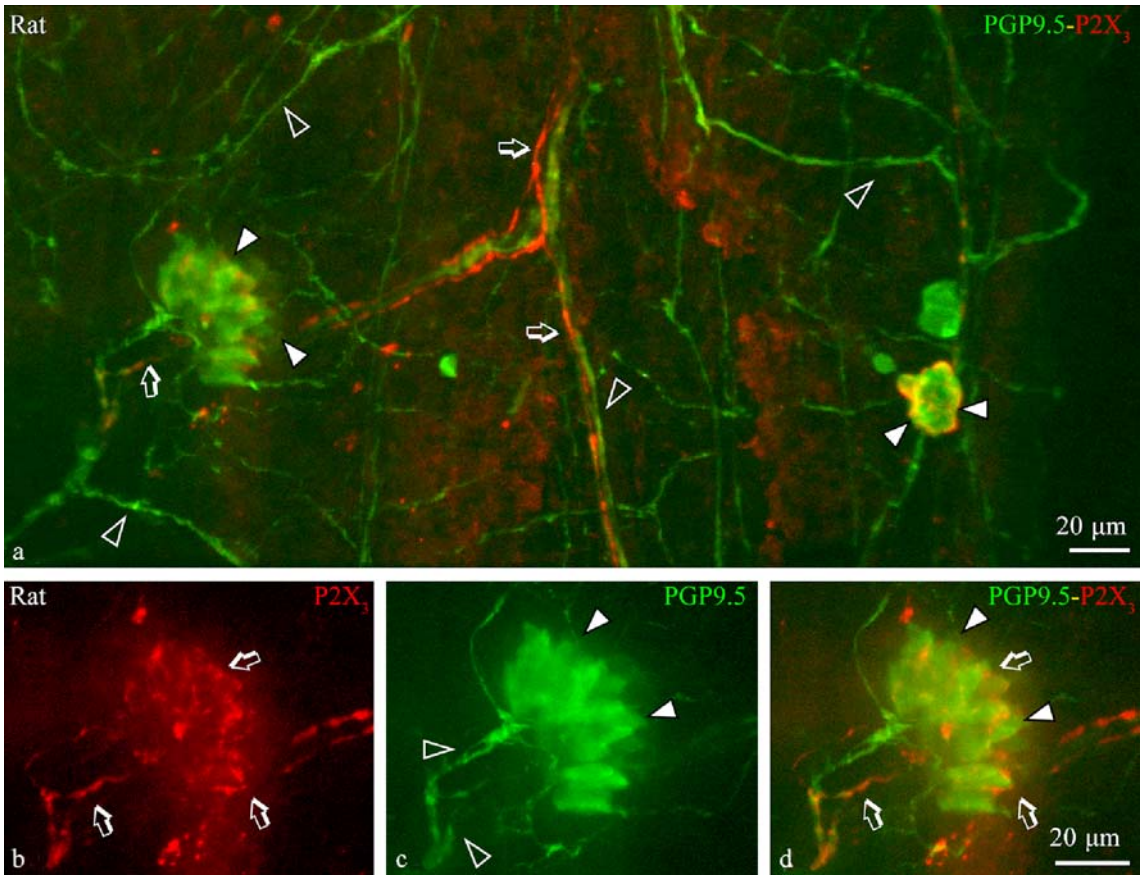

Fig. 12 Confocal images of a rat lung vibratome slice (PD10) immunostained for the ATP receptor $P2X_3$ (*red* Cy3 fluorescence) and the neuronal marker PGP9.5 (*green* FITC fluorescence). **a** Overview of a tangential section of a bronchial wall showing a complex network of PGP9.5-IR nerve fibres (*open arrowheads*). In addition, a subpopulation of nerve fibres displays clear immunoreactivity for the $P2X_3$ receptor (*open arrows*). In particular, pulmonary NEBs, also stained for PGP9.5, appear to be contacted by $P2X_3$-IR nerve terminals (*arrowheads*). Projection of 16 confocal images (5-µm intervals). **b**–**d** Details of one of the NEBs seen in **a**. All images originate from a projection of 100 confocal images (0.5-µm intervals). **b** *Red* channel revealing abundant intraepithelial $P2X_3$-receptor-IR vagal sensory nerve endings (*open arrows*). **c** *Green* channel showing a PGP9.5-IR NEB (*white arrowheads*) selectively contacted by PGP9.5-IR nerve fibres (*open arrowheads*). **d** Combination of both channels shows that the extensive intraepithelial arborisation of $P2X_3$-IR nerve terminals (*open arrows*) coincides with the presence of a pulmonary NEB (*white arrowheads*).

The vital dye, neutral red, has been used to label NEBs in lung slices (Fu et al. 1999, 2000, 2001, 2002). In our study, however, NEB cells of mice and rats could only be identified in living lung slices with difficulty when neutral red was used and certainly not reproducibly. Although the

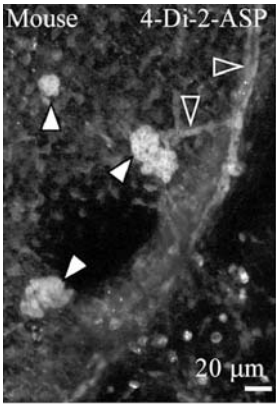

Fig. 13 Tangential section of the mucosal layer of a bronchiole in a lung slice of a 7-day-old mouse revealing three brightly 4-Di-2-ASP-fluorescent intraepithelial cell groups (*arrowheads*). Note that nerve fibres (*open arrowheads*), which make contact with a labelled cell group, are also stained with 4-Di-2-ASP. Projection of 12 confocal images (2-µm intervals)

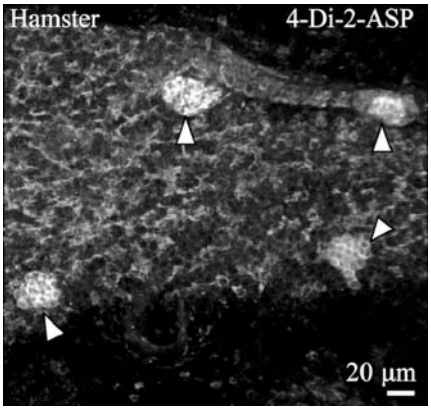

Fig. 14 After 4-Di-2-ASP staining, distinct intensely fluorescent cell groups (*arrowheads*), can easily be distinguished between the epithelial cells of a tangentially sectioned bronchus in a lung slice of a 5-day-old hamster. Projection of 17 confocal images (2-µm intervals)

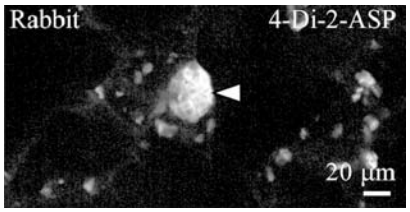

Fig. 15 Intensely fluorescent cell group (*arrowhead*) located in a respiratory area of a rabbit lung slice (4-week-old), as seen after 4-Di-2-ASP staining. Projection of seven confocal images (2-µm intervals)

exact staining mechanism of neutral red is still uncertain, uptake of the dye may be dependent upon the accumulation of 5-HT (Stuart et al. 1974). Since 5-HT is apparently only present at low concentrations in NEBs of rat lungs (own unpublished observations; Cutz et al. 1974), it is not surprising that labelling NEBs with neutral red is difficult in living rat lung slices. Even the pretreatment of mice and rats with 5-HT precursors only yields poor neutral red staining of NEB cells and does not result in reproducible visualisation. This is in contrast to rabbit NEB cells, which show good immunoreactivity for 5-HT (Hage 1976; Sorokin and Hoyt 1989) and appear to stain well with neutral red (Youngson et al. 1993; Fu et al. 1999, 2002). Moreover, because faint neutral red staining in airway epithelium does not always correspond to the presence of a PGP9.5-IR NEB in rat, this staining should be interpreted with great caution, as should the results from further physiological studies based on such staining.

Labelling by 4-Di-2-ASP, in combination with PGP9.5 immunostaining after fixation, has confirmed that neuronal somata located in intrinsic ganglia and nerve terminals contacting NEBs are still intact in lung slices after 4–8 h in vitro. Because the nerve endings associated with pulmonary NEBs are agreed to have direct effects on the response of these NEBs to stimuli (Lauweryns and Van Lommel 1986; Adriaensen et al. 2003), the present lung slice model offers an excellent opportunity for performing in vitro studies on NEBs that are still connected to their complex innervation.

Although 4-Di-2-ASP visualises pulmonary NEBs in rats, mice, hamsters and rabbits, the uptake rate of 4-Di-2-ASP appears to differ among the examined species, ranging from 1 h in hamster to 6 h in murine slices. As the uptake of this dye has been assessed to be directly related to some aspects of cell metabolism (Magrassi et al. 1987; Hanani 1992; Cornelissen et al. 1996), slight species differences in the activity of PNECs may be responsible for the observed differences in the accumulation times of 4-Di-2-ASP. Comparable to our observations in NEBs, 4-Di-2-ASP fluorescence has been demonstrated to remain detectable in neurons of the choroid and nerve fibres of the enteric nervous system for several hours after incubation (Lichtman et al. 1987; Hanani 1992; Bergua et al. 1994). 4-Di-2-ASP-labelled cells have been reported to be useful in long-term in vivo experimental set-ups (Magrassi et al. 1987; Lichtman et al. 1987; Herrera and Banner 1990). The latter is in agreement with our experiments confirming the adequate viability of 4-Di-2-ASP-stained NEB cells in lung slices.

Although none of the nuclei of NEB cells reveals PI fluorescence after the viability test, the lung slices harbour a considerable number of PI-stained nuclei. PI viability testing is based on healthy living cells possessing an intact cell membrane that is impermeable to PI. During the cutting of vibratome slices, many of the extensive thin processes of pneumocytes and extensions of smooth muscle cells and other cell types are inevitably damaged. Airway epithelium, including NEBs, on the other hand, is mainly composed of compact polygonal cells. Some of the latter will undoubtedly also be sectioned. However, this damage is most likely fatal and the cells therefore completely disappear, resulting in the absence of nuclear PI staining.

Although the intracellular localisation of stryryl pyridinium dyes in general has still not been completely elucidated (Magrassi et al. 1987; Cornelissen et al. 1996), the involvement of a membranous compartment is proba-

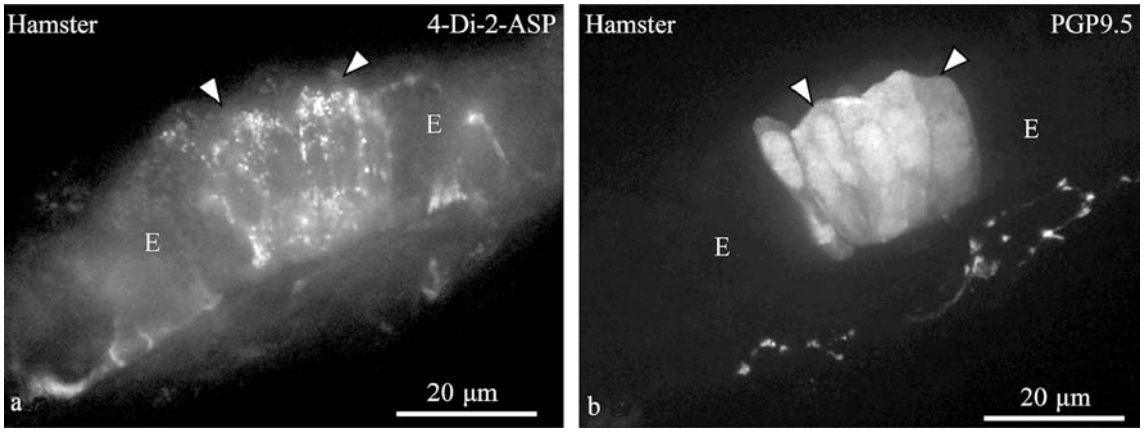

Fig. 16 **a** View of a group of fluorescent cells (*arrowheads*) between unstained epithelial cells (*E*) of a bronchus as seen after 4-Di-2-ASP staining in a hamster lung slice (PD4). Projection of 30 confocal images (0.5-µm intervals). **b** Subsequent immunostaining for PGP9.5 on the fixed lung slice demonstrating that the 4-Di-2-ASP-stained cell group in **a** coincides with the presence of a PGP9.5-IR pulmonary NEB (*arrowheads*). Projection of 35 confocal images (0.5-µm intervals)

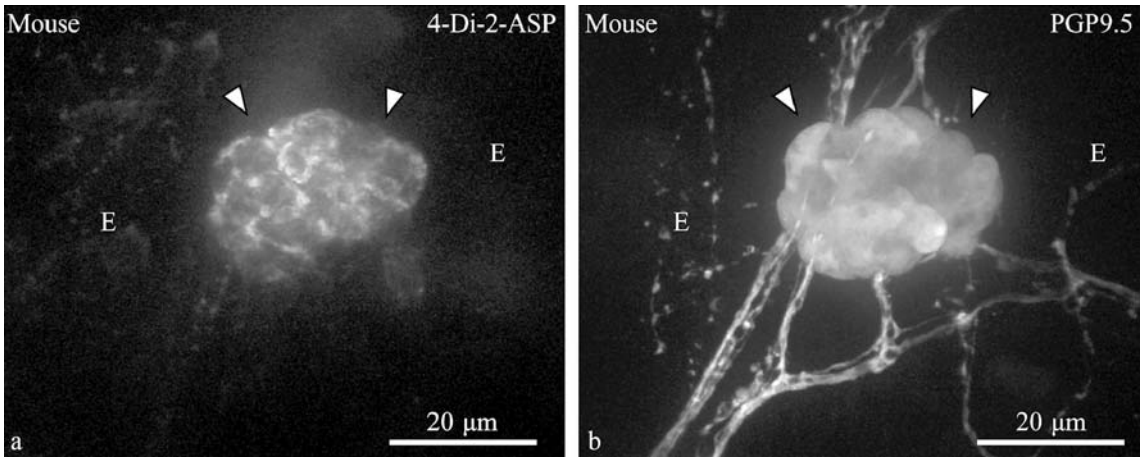

Fig. 17 High-magnification detail of a tangential section through the wall of a bronchus in a murine (PD7) lung slice. **a** 4-Di-2-ASP fluorescence (*arrowheads*) appears to be selectively taken up by an intraepithelial cell group (*E* epithelium). Projection of 50 confocal images (0.5-µm intervals). **b** Fixation and immunocytochemistry for PGP9.5 confirm that the fluorescent cell group seen in **a** is indeed a pulmonary NEB (*arrowheads*). Projection of 55 confocal images (0.5-µm intervals)

ble, because these dyes belong to a voltage-sensitive class that appears to be taken up in plasma membranes of excitable cells (Loew et al. 1985) and subsequently in mitochondria (Rafael and Nicholls 1984). The recorded movement of 4-Di-2-ASP-fluorescent particles in NEB cells most likely corresponds to the motion of mitochondria. Rat NEB cells are known to have a high nucleus/cytoplasm index and contain only a few, small, round to oval mitochondria (Van Lommel and Lauweryns 1993). In our experiments, the morphological appearance of mitochondria is identical if compared immediately after staining and after 24 h. As the activity of mitochondria is related to the viability of the cells, our observations indicate that NEB cells are healthy and dynamic after incorporation of the 4-Di-2-ASP dye.

In the literature, conflicting findings have been reported regarding the phototoxic effects of the illumination of 4-Di-2-ASP-labelled cells, varying from clearly negative effects of intense exposure in the frog neuromuscular junction (Herrera and Banner 1990) to no obvious effects on the function of mouse motor nerve terminals (Magrassi et al. 1987) and the electrophysiological characteristics of myenteric neurons in the gut (Hanani 1992; Cornelissen et al. 1996). In view of the possible phototoxic effects of the sustained excitation and emission of 4-Di-2-ASP in NEB cells, the viability of the cells has been verified and found to be unaffected after time-lapse imaging over a period of 10 min under continuous excitation in our experimental set-up. The UltraVIEW LCI dual spinning disk confocal microscope employed for all imaging in the present study has been specifically designed for live cell imaging, allowing the fast capturing of high-resolution images with minimal photobleaching and low phototoxicity.

Comparison of the immunostaining of fixed lung slices with the results previously obtained in cryostat sections of rat lungs (Brouns et al. 2000, 2003a) has yielded no obvious differences. Since the present $P2X_3$ immunostaining has been performed by using TSA, we have concluded that the staining enhancement protocol, previously described for cryostat sections, can also be used for fixed vibratome lung slices (200–300 µm thick). This observa-

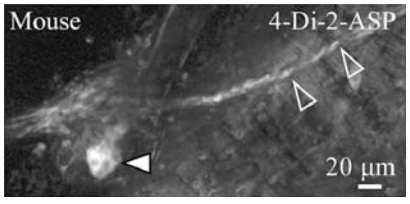

Fig. 18 In addition to the intraepithelial labelled NEBs, other fluorescent cells with a non-epithelial location (*arrowhead*) can be found in the wall of airways in lung slices after in vitro incubation with 4-Di-2-ASP. Images of a bronchus in a murine (PD7) lung slice. Note the stained nerve fibres in the neighbourhood of the 4-Di-2-ASP-fluorescent cells (*open arrowheads*). Projection of 70 confocal images (1-µm intervals)

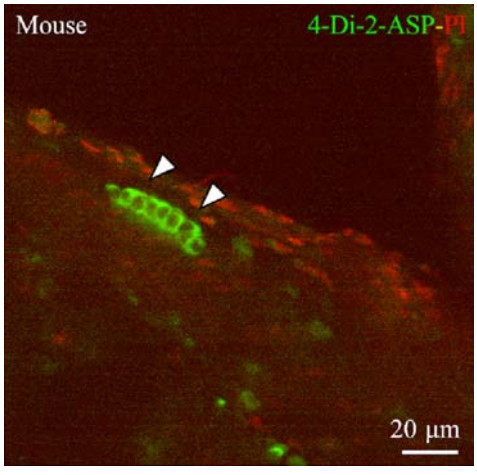

Fig. 19 PI (*red* fluorescence) staining of a murine lung slice (PD 11) 8 h after 4-Di-2-ASP (*green* fluorescence) incubation, demonstrating that none of the 4-Di-2-ASP-fluorescent epithelial cells that belong to a pulmonary NEB (*arrowheads*), exhibit nuclear PI staining. Some other cells, outside the airway epithelium however show nuclear PI staining. Projection of 25 confocal images (1-µm intervals)

tion is important for future combined physiological and morphological studies, because several of the immunocytochemical methods used to visualise the numerous populations of delicate nerve terminals that selectively contact NEBs in rat lungs require procedures for enhancement of the immunostaining (Brouns et al. 2002, 2003b, 2004).

In conclusion, this is the first report that characterises the styryl pyridinium dye 4-Di-2-ASP as a selective fluorescent label for pulmonary NEBs in living lung slices. The clear easy reproducible visualisation of intact living NEBs in an in vitro lung slice model offers great opportunities to monitor and manipulate NEB cells and their complex innervation directly in a fluorescent "live cell imaging" set-up or in electrophysiological experiments. Because the reported 4-Di-2-ASP staining of NEBs appears to be reliable and reproducible for lung slices of several animal species, the selection of an animal model is no longer limited. The presence of nerve endings and intrinsic neuronal cell bodies in the slices should also enable the study of interactions between NEBs and nerve terminals. The proposed lung slice model and 4-Di-2-ASP staining of NEBs clearly open new perspectives for further functional studies of pulmonary NEBs.

Acknowledgements We are grateful to Prof. G. Burnstock (Director of the Autonomic Neuroscience Institute, Royal Free and University College Medical School, London, UK) for his invaluable input in the ATP receptor studies. We thank H. De Pauw, R. Spillemaeckers, G. Svensson, F. Terloo and G. Vermeiren for technical assistance, J. Van Daele and D. De Rijck for help with microscopy, imaging and illustrations, D. Vindevogel for aid with the manuscript, and S. Kockelberg for secretarial help.

References

Adriaensen D, Scheuermann DW (1993) Neuroendocrine cells and nerves of the lung. Anat Rec 236:70–85

Adriaensen D, Timmermans J-P (2004) Purinergic signalling in the lung: important in asthma and COPD? Curr Opin Pharmacol 4:207–214

Adriaensen D, Brouns I, Van Genechten J, Timmermans J-P (2003) Functional morphology of pulmonary neuroepithelial bodies: extremely complex airway receptors. Anat Rec 270A:25–40

Bergua A, Neuhuber WL, Naumann GOH (1994) Visualization of human choroidal ganglion cells with the supravital fluorescent dye 4-(4-diethylaminostyryl)-*N*-methylpyridium iodide. Ophthalmic Res 26:290–295

Brouns I, Adriaensen D, Burnstock G, Timmermans J-P (2000) Intraepithelial vagal sensory nerve terminals in rat pulmonary neuroepithelial bodies express $P2X_3$ receptors. Am J Respir Cell Mol Biol 23:52–61

Brouns I, Van Genechten J, Scheuermann DW, Timmermans J-P, Adriaensen D (2002) Neuroepithelial bodies: a morphologic substrate for the link between neuronal nitric oxide and sensitivity to airway hypoxia? J Comp Neurol 449:343–354

Brouns I, Van Genechten J, Burnstock G, Timmermans J-P, Adriaensen D (2003a) Ontogenesis of P2X3 receptor-expressing nerve fibres in the rat lung, with special reference to neuroepithelial bodies. Biomed Res 14:80–86

Brouns I, Van Genechten J, Hayashi H, Gajda M, Gomi T, Burnstock G, Timmermans J-P, Adriaensen D (2003b) Dual sensory innervation of pulmonary neuroepithelial bodies. Am J Respir Cell Mol Biol 28:275–285

Brouns I, Pintelon I, Van Genechten J, De Proost I, Timmermans J-P, Adriaensen D (2004) Vesicular glutamate transporter 2 is expressed in different nerve fibre populations that selectively contact pulmonary neuroepithelial bodies. Histochem Cell Biol 121:1–12

Carabba VH, Sorokin SP, Hoyt RFJ (1985) Development of neuroepithelial bodies in intact and cultured lungs of fetal rats. Am J Anat 173:1–27

Cho T, Chan W, Cutz E (1989) Distribution and frequency of neuroepithelial bodies in post-natal rabbit lung: quantitative study with monoclonal antibody against serotonin. Cell Tissue Res 255:353–362

Cornelissen W, Timmermans J-P, Van Bogaert P-P, Scheuermann DW (1996) Electrophysiology of porcine myenteric neurons revealed after vital staining of their cell bodies. A preliminary report. Neurogastroenterol Mot 8:101–109

Cutz E, Jackson A (1999) Neuroepithelial bodies as airway oxygen sensors. Respir Physiol 115:201–214

Cutz E, Chan W, Wong V, Conen PE (1974) Endocrine cells in rat fetal lungs. Ultrastructural and histochemical study. Lab Invest 30:458–464

Cutz E, Yeger H, Wong V, Bienkowski E, Chan W (1985) In vitro characteristics of pulmonary neuroendocrine cells isolated from rabbit fetal lung. I. Effects of culture media and nerve growth factor. Lab Invest 53:672–683

Fu XW, Nurse CA, Wang YT, Cutz E (1999) Selective modulation of membrane currents by hypoxia in intact airway chemoreceptors from neonatal rabbit. J Physiol (Lond) 514:139–150

Fu XW, Wang D, Nurse CA, Dinauer MC, Cutz E (2000) NADPH oxidase is an O_2 sensor in airway chemoreceptors: evidence from K^+ current modulation in wild-type and oxidase-deficient mice. Proc Natl Acad Sci USA 97:4374–4379

Fu XW, Wang D, Pan J, Farragher SM, Wong V, Cutz E (2001) Neuroepithelial bodies in mammalian lung express functional serotonin type 3 receptor. Am J Physiol Lung Cell Mol Physiol 281:L931–L940

Fu XW, Nurse CA, Wong V, Cutz E (2002) Hypoxia-induced secretion of serotonin from intact pulmonary neuroepithelial bodies in neonatal rabbit. J Physiol (Lond) 539:503–510

Hage E (1976) Endocrine-like cells of the pulmonary epithelium. In: Coupland RE, Fujita T (eds) Chromaffin, enterochromaffin and related cells. Elsevier, Amsterdam, pp 317–332

Hanani M (1992) Visualization of enteric and gallbladder ganglia with a vital fluorescent dye. J Auton Nerv Syst 38:77–84

Herrera AA, Banner LR (1990) The use and effects of vital fluorescent dyes: observation of motor nerve terminals and satellite cells in living frog muscles. J Neurocytol 19:67–83

Hillsley K, Jennings LJ, Mawe GM (1998) Neural control of the gallbladder: an intracellular study of human gallbladder neurons. Digestion 59:125–129

Kelly SS, Anis N, Robbins N (1985) Fluorescent staining of living mouse neuromuscular junctions. Pflügers Arch 404:97–99

Kemp PJ, Lewis A, Hartness M, Searle GJ, Miller P, O'Kelly I, Peers C (2002) Airway chemotransduction: from oxygen sensor to cellular effector. Am J Respir Crit Care Med 166:S17–S24

Lauweryns JM, Peuskens JC (1972) Neuro-epithelial bodies (neuroreceptor or secretory organs?) in human infant bronchial and bronchiolar epithelium. Anat Rec 172:471–481

Lauweryns JM, Van Lommel A (1986) Effect of various vagotomy procedures on the reaction to hypoxia of rabbit neuroepithelial bodies: modulation by intrapulmonary axon reflexes. Exp Lung Res 11:319–339

Lichtman JW, Magrassi L, Purves D (1987) Visualization of neuromuscular junctions over periods of several months in living mice. J Neurosci 7:1215–1222

Loew LM, Cohen LB, Salzberg BM, Obaid AL, Bezanilla F (1985) Charge-shift probes of membrane potential. Characterization of aminostyrylpyridinium dyes on the squid giant axon. Biophys J 47:71–77

Magrassi L, Purves D, Lichtman JW (1987) Fluorescent probes that stain living nerve terminals. J Neurosci 7:1207–1214

Nurse CA, Farraway L (1989) Characterization of Merkel cells and mechanosensory axons of the rat by styryl pyridinium dyes. Cell Tissue Res 255:125–128

Peers C, Kemp PJ (2001) Acute oxygen sensing: diverse but convergent mechanisms in airway and arterial chemoreceptors. Respir Res 2:145–149

Rafael J, Nicholls DG (1984) Mitochondrial membrane potential monitored in situ within isolated guinea pig brown adipocytes by a styryl pyridinium fluorescent indicator. FEBS Lett 170: 181–185

Scheuermann DW (1987) Morphology and cytochemistry of the endocrine epithelial system in the lung. Int Rev Cytol 106:35–88

Schrödl F, De Laet A, Tassignon MJ, Van Bogaert P-P, Brehmer A, Neuhuber WL, Timmermans J-P (2003) Intrinsic choroidal neurons in the human eye: projections, targets and basic electrophysiological data. Invest Ophthalmol Vis Sci 44:3705–3712

Sorokin SP, Hoyt RF (1989) Neuroepithelial bodies and solitary small-granule cells. In: Massaro D (ed) Lung cell Biology. Dekker, New York, pp 191–344

Speirs V, Cutz E (1993) An overview of culture and isolation methods suitable for in vitro studies on pulmonary neuroendocrine cells. Anat Rec 236:35–40

Speirs V, Wang YV, Yeger H, Cutz E (1992) Isolation and culture of neuroendocrine cells from fetal rabbit lung using immunomagnetic techniques. Am J Respir Cell Mol Biol 6:63–67

Stuart AE, Hudspeth AJ, Hall ZW (1974) Vital staining of specific monoamine-containing cells in the leech nervous system. Cell Tissue Res 153:55–61

Van Genechten J, Brouns I, Burnstock G, Timmermans J-P, Adriaensen D (2004) Quantification of neuroepithelial bodies and their innervation in fawn–hooded and Wistar rat lungs. Am J Respir Cell Mol Biol 30:20–30

Van Lommel A, Lauweryns JM (1993) Neuroepithelial bodies in the fawn hooded rat lung: morphological and neuroanatomical evidence for a sensory innervation. J Anat 183:553–566

Wasano K, Yamamoto T (1978) Monoamine-containing granulated cells in the frog lung. Cell Tissue Res 193:201–209

Widdicombe JG (2001) Airway receptors. Respir Physiol 125:3–15

Youngson C, Nurse C, Yeger H, Cutz E (1993) Oxygen sensing in airway chemoreceptors. Nature 365:153–155

Youngson C, Nurse C, Yeger H, Curnutte JT, Vollmer C, Wong V, Cutz E (1997a) Immunocytochemical localization on O_2-sensing protein (NADPH oxidase) in chemoreceptor cells. Microsc Res Tech 37:101–106

Youngson C, Nurse CA, Wang D, Cutz E (1997b) Ionic currents and oxygen-sensing mechanism in neuroepithelial body cells. In: Cutz E (ed) Cellular and molecular biology of airway chemoreceptors. Landes Bioscience, Austin, pp 71–108